Correlation between high ratio of circulating PMN-MDSCs and poor prognosis in metastatic hormone sensitive prostate cancer

Yuki Kohada
Division of Urology, Faculty of Medicine, Tohoku Medical and Pharmaceutical University
Akito Kuromoto
Division of Urology, Faculty of Medicine, Tohoku Medical and Pharmaceutical University
Kazuya Takeda
Division of Immunology, Faculty of Medicine, Tohoku Medical and Pharmaceutical University
Yuri Atobe
Division of Neurology, Faculty of Medicine, Tohoku Medical and Pharmaceutical University
Jun Ito
Division of Urology, Faculty of Medicine, Tohoku Medical and Pharmaceutical University
Tomonori Kaifu
Division of Immunology, Faculty of Medicine, Tohoku Medical and Pharmaceutical University
Yasuhiro Kaiho
Division of Urology, Faculty of Medicine, Tohoku Medical and Pharmaceutical University
Ichiro Nakashima
Division of Neurology, Faculty of Medicine, Tohoku Medical and Pharmaceutical University
Nobuyuki Hinata
Department of Urology, Hiroshima University Graduate School of Biomedical Sciences
Akira Nakamura (aki-n@tohoku-mpu.ac.jp)
Division of Immunology, Faculty of Medicine, Tohoku Medical and Pharmaceutical University
Makoto Sato
Division of Urology, Faculty of Medicine, Tohoku Medical and Pharmaceutical University

Research Article

Keywords: Myeloid-Derived Suppressor Cells, Prostatic Neoplasms, Androgen Receptor Antagonists, Flow Cytometry, Single-Cell Analysis, Sequence Analysis, RNA

Posted Date: March 16th, 2022

DOI: https://doi.org/10.21203/rs.3.rs-1452049/v1

Abstract

Introduction: This study aims to investigate the role of myeloid-derived suppressor cells (MDSCs) in metastatic-hormone sensitive prostate cancer (mHSPC).

Materials and methods: MDSC subsets in peripheral blood samples were classified and evaluated by flow cytometry into early MDSCs (e-MDSCs), polymorphonuclear MDSCs (PMN-MDSCs), and monocytic MDSCs (M-MDSCs). Prostate-specific antigen progression free survival (PSA–PFS) and overall survival (OS) were evaluated to assess the prognostic value of each of the MDSC subsets. The immune cell dynamics and gene expression alteration were analyzed by single cell RNA sequencing (scRNA-seq) in the representative case.

Results: Thirty-one patients with mHSPC and eleven healthy controls (HCs) were included in this study. In patients with mHSPC, PMN/M-MDSCs were significantly higher than those of HCs ($p < 0.05$) before treatment and declined to almost the same level as in the HCs after treatment. Although there were no differences between high and low ratio of e-MDSCs and M-MDSCs, patients with a high ratio of PMN-MDSCs (≥ 0.30%) displayed a lower PSA–PFS and OS than those with a low ratio (< 0.30%) ($p < 0.05$). The analysis of scRNA-seq showed that the expression of genes implicated in tumor progression was upregulated in a representative mHSPC case.

Conclusion: The high frequency of PMN-MDSCs correlated with poor prognosis in patients with mHSPC. PMN-MDSCs and their highly expressed genes are included as potential novel therapeutic targets for mHSPC.

Introduction

Together with lung and colorectal cancer, prostate cancer (PC) is one of the three most common cancers among men. Metastatic PC is only 6% in all newly diagnosed PC patients, but has a poor prognosis, with a 5-year relative survival rate of only 30% [1]. Androgen deprivation therapy (ADT), which is the primary treatment of metastatic PC, provides temporary disease control in the majority of patients [2]. Within two years, however, more than half of patients with metastatic PC progress to castration-resistance prostate cancer (CRPC), which is refractory to ADT [3]. The prognosis of CRPC is still poor even with other treatments, including taxane chemotherapy. Various immunotherapies widely used in other cancers have been tried to improve the prognosis of metastatic PC patients, such as immune checkpoint inhibitors [4]. Despite this, there are still no approved therapies for PC except for an autologous dendritic cell vaccine called sipuleucel-T [5]. In order to establish a novel effective treatment, it is necessary to investigate how immunotherapy-resistance metastatic PC affects the host immune system.

Myeloid-derived suppressor cells (MDSCs) are the immunosuppressive immature myeloid cells that are expanded in the tumor-bearing condition [6]. MDSCs are heterogenous immature myeloid cells which can be divided into three representative subsets based on their phenotypic and morphological characteristics [7]. Polymorphonuclear MDSCs (PMN-MDSCs) and monocytic MDSCs (M-MDSCs) are

phenotypically and morphologically similar to neutrophil and monocyte, respectively. The immature subsets of MDSCs, which lack monocytic and granulocytic markers are called early-stage MDSCs (e-MDSCs). Each of the MDSC subsets are not only phenotypically and morphologically distinct, but also have unique functional characteristics and biochemical traits that suppress the anti-tumor immunity in tumor-associated immune system. For example, PMN-MDSCs have been reported to enhance angiogenesis through the production of matrix metallopeptidase (MMP)-9 and the vascular endothelial growth factor (VEGF), and also to have a suppressive effect against T cells [8]. M-MDSCs have been shown to differentiate into tumor associated macrophages (TAMs) after migration to the tumor site, and act to play an immunosuppressive role [9]. In head and neck canner and ovarian cancer, it has been reported that e-MDSCs have an immunosuppressive property, but their specific roles are still uncertain in other tumors [10]. It has been reported that the high frequency of MDSCs in peripheral blood is associated the disease progression and poor prognosis of many malignant neoplasms, including lung cancer and gastric cancer [11, 12]. The several studies which have shown the role of MDSCs in localized PC or CRPC have been mainly focused on either PMN-MDSCs or M-MDSCs, however, there have been no reports on the involvement of the three MDSC subsets in untreated metastatic PC patients [13-16].

In this study, to investigate which of the MDSC subtypes is associated with tumor progression and the poor prognosis in pre-treated metastatic PC, we analyzed three types of MDSCs in the periphery before and after treatment with a GnRH antagonist and clarified the correlation between each of the MDSC subsets ratios with PFS and OS in metastatic-hormone sensitive prostate cancer (mHSPC). We also analyzed the immune cell dynamics and gene expression alteration by single cell RNA-sequencing (scRNA-seq) in the representative case. We found that PMN-MDSC fractions were correlated with a poor prognosis in mHSPC patients, and the different immune cell subsets and immunosuppressive gene expression of PMN-MDSCs in the data of the scRNA-seq suggested PMN-MDSCs are implicated in the response to ADT for mHSPC.

Subjects/patients And Methods

Patient population and study design

The present study was a prospective analysis of data acquired from patients with newly diagnosed mHSPC between 2017 and 2021. This study was approved by the clinical research ethics board of Tohoku Medical and Pharmaceutical Hospital. All patients were diagnosed with metastatic prostate cancer because metastatic findings were detected in the lymph node outside the pelvis, bone, and viscera, and the following were determined by pathological and clinical tests: biopsy Gleason score; neutrophile, lymphocyte and monocyte counts; and the levels of prostate-specific antigen (PSA), alkaline phosphatase (ALP), lactate dehydrogenase (LDH), hemoglobin (Hb) and albumin (Alb). PSA progression was defined as a first increase in PSA greater than 25% and > 2 ng/mL above nadir based on the Prostate Cancer Clinical Trials Working Group 3 [17]. PSA progression-free survival (PSA-PFS) was defined as the duration between the start of ADT to PSA progression. Patients showing normalized PSA levels after 3 months of ADT with GnRH agonist (degarelix) were diagnosed with mHSPC and were included in this study. The

patients' characteristics are detailed in Table 1 and Supplementary (Suppl.) Table 1. Eleven healthy volunteers (median; 41, range; 24–52) served as normal controls.

PBMCs isolation and Flowcytometric analysis of MDSC subsets

Blood samples (4 mL) from the patients were drawn into heparin blood collection tubes and processed within 2 hours. After the removal of red blood cells (RBCs) using HetaSep (STEMCELL Technologies, Vancouver, Canada), the peripheral blood cells (PBMCs) were enriched by density gradient centrifugation (TOMY, Tokyo, Japan) at 90 x g for 4 minutes at room temperature. PBMCs were isolated from the interface and washed in 35 ml of phosphate-buffered saline (PBS). The solution was centrifuged at 120 x g for 11 minutes by density centrifugation.

The fractions of MDSCs in the peripheral blood was tested by using Flow cytometry (Attune NxT Flow Cytometer, Thermo Fisher Scientific, Waltham, MA). Flow cytometry was conducted using the following antibodies [7]: anti-CD3-FITC (UCHT1, eBioscience, San Diego, CA.), anti-CD11b-Super Bright436 (ICRF44, eBioscience), anti-CD14-PE-Cy5 (61D3, eBioscience), anti-CD15-Brilliant Violet711 (W6D3, Biolegend, Sandiego, CA.), anti-CD19-FITC (HIB19, Tonbo Biosciences, Sandiego, CA.), anti-CD33-PE (WM53, eBioscience), anti-CD45-PerCP/Cy5.5 (HI30, Biolegend,), anti-CD56-FITC (TULY56, Thermo, Tokyo, Japan), anti-HLA-DR-APC-eFluor780 (LN3, eBioscience). The data of 10,000–100,000 events were analyzed using the FlowJo software programs (BD bioscience, San Jose, CA). The MDSC subsets were defined as following surface markers [6]: M-MDSCs; $CD11b^{+}CD15^{-}CD14^{+}HLA\text{-}DR^{-}$, PMN-MDSCs; $CD11b^{+}CD14^{-}CD15^{+}$, e-MDSCs; $CD11b^{+}CD33^{+}CD15^{-}CD14^{-}$Lineage $(CD3/19/\ 56)^{-}$ $HLA\text{-}DR^{-}$. The proportions of each MDSC subsets calculated using CD45-positive cell fraction.

Single-cell RNA sequence and data analysis

An scRNA-seq of gene expression and immune cell profiling analysis were performed using the 10X Genomics Chromium Single Cell platform according to the manufacturer's instructions. Briefly, RBC removal PBMCs were capsulized using microfluidics technology, and were then barcoded by a unique molecular identifier (UMI). complementary DNA was sequenced on an Illumina 3000 HiSeq system. Raw reads were aligned to the GRCh38 human transcriptome using STAR (Spliced Transcripts Alignment to a Reference) and gene expression was quantified by the Cell Ranger software package (version 5.0.0) with default parameters. The total number of cells passing the filters was 3,885 cells for the patient and 4,800 cells for the healthy subject, with 21, 697 and 21, 280 genes, respectively, which were passed the quality control check. We compressed the dimensions using T-distributed stochastic neighbor embedding (t-SNE) and plotted the single cells in two dimensions. Data were log-normalized for expression levels and scaled around zero to calculate the relative expression of the genes.

Statistical Analysis

Differences in variables with a continuous distribution across dichotomous categories were assessed using the Wilcoxon signed-rank test. Spearman's rank correlation coefficient was used to assess the

respective correlations between each MDSC sub-domains and clinicopathological factors. PSA-PFS and overall survival (OS) were estimated using the Kaplan–Meier method. All statistical analyses were conducted using JMP pro 16.0.0 (SAS Institute Inc., Cary, NC, USA), with $p < 0.05$ indicating statistical significance.

Results

Parallel fluctuation of circulating PMN-MDSCs and M-MDSCs in patients with mHSPC in response to ADT

We investigated three MDSC subsets, e-MDSCs, PMN-MDSCs, and M-MDSCs from PBMCs in patients with newly diagnosed mHSPC. In a total of 74 metastatic PC patients, 43 patients were excluded for the following reasons: they were CRPC patients, had no prostatic biopsy or did not consent to this study. A total of 31 patients with untreated metastatic PC patients were included in this study (Fig. 1). We first evaluated the therapeutic effect of ADT in patients with untreated metastatic PC and confirmed that all patients were sensitive to hormonal therapy. As shown in Suppl. Fig. 1, the PSA levels in all 31 patients declined from pre-ADT to 3 months post-treatment, indicating that all subjects were mHSPC. Fig. 2-A shows the representative dot plots for one of the patients in the study to illustrate the gating strategy. Since an expansion of MDSCs has been reported in patients with diabetes and also in smokers [18, 19], this was considered in the population of MDSCs in this study. No effect on MDSC frequencies from either diabetes or smoking was found in the subjects in our study (Suppl. Fig. 2). We next investigated the cell fractions from hormone-sensitive patients before and 3 months after treatment. As shown in Fig. 2-B, while there was no significant difference in the e-MDSC subset between mHSPC patients (median value :0.76%) and the healthy control (0.67%), the PMN/M-MDSC fraction was significantly elevated in patients relative to the controls before the treatment (PMN-MDSCs: 0.28% vs 0.11%, M-MDSCs: 1.46% vs 0.58%) (Fig. 2-B). The percentage of PMN/M-MDSCs in patients declined to almost the same level as in the healthy subjects after treatment, suggesting that these MDSC subsets fluctuated in conjunction with the therapeutic effects of the GnRH antagonist.

Relevance of MDSC fractions with serological and hematological examination

While it has been reported that PSA levels are associated with the frequencies of M-MDSCs [14, 16], their correlation with e-MDSCs and/or PMN-MDSCs has not been investigated in PC patients. Furthermore, there are no reports showing an association between each MDSC subset and other serological/hematological tests in PC patients. Therefore, we investigated the correlation between each of the MDSC subsets and the results of serological and hematological examinations (PSA, ALP, LDH, peripheral blood factions, biopsy Gleason score) in patients with mHSPC at the start of the treatment (Fig 3, and Suppl. Fig. 2, 3). The frequency of e-MDSCs did not correlate with serum PSA and ALP levels, but not with PSA levels. M-MDSC fractions correlated with PSA levels as previously reported [14, 16], in addition to ALP levels. MDSC have been reported to differentiate into osteoclast-like cells and cause bone destruction in mice with bone metastatic carcinoma [20], which may be reflected in the correlation with increased ALP levels. On the other hand, no correlation was found between the percentages of

neutrophils, monocytes, and lymphocytes and the ratios of each of the MDSC subsets. According to these results, there is a clear correlation between PMN-MDSC and M-MDSC frequencies and the PSA and/or ALP levels in patients with newly diagnosed mHSPC.

Prognostic value of MDSCs for patients with mHSPC

The high frequency of MDSCs was shown to be associated with a poor prognosis with various malignant neoplasms via the immunosuppressive effect in the tumor-associated immune system [11, 12]. While the association between the total MDSC subsets and OS in PC patients has been reported in an earlier study [15], no studies have examined the impact of each of the MDSC subsets on the prognosis of patients with mHSPC. Therefore, we assessed the prognostic value of pretreatment MDSCs in mHSPC patients (The mean follow-up time: 567 days). During the follow-up period, 19 patients with mHSPC had PSA progression, and 3 patients expired due to tumor aggravation. In order to evaluate the prognostic value of MDSCs, we compared mHSPC patients with high and low percentages of each of the MDSC subsets. While cut-off values from retrospective studies have been used in previous studies [21, 22], it is necessary to set a more sensitive cut-off value for a prospective therapeutic intervention study in untreated subjects. We determined the cut-off value for the high percentage of PMN-MDSCs and M-MDSCs, except for e-MDSCs, at three times the median value of normal subjects, and a value well above the standard deviation (SD) of normal subjects. The cut-off value for the high percentage of e-MDSCs was set to be approximately above median values of the patient's e-MDSCs because there were no significant differences between patients and healthy subjects. Therefore, we specifically defined the following values as cut off values for each of the MDSC subsets: e-MDSCs 0.75%, PMN-MDSCs 0.30%, M-MDSCs 1.70%. As shown in Fig. 4-A, patients with a high ratio of PMN-MDSCs displayed a lower PSA–PFS than those with a low ratio. In addition, a high frequency of PMN-MDSCs was associated with a lower OS in subjects (Fig. 4-B). However, high percentages of e-MDSCs and/or M-MDSCs did not relate with PSA–PFS and OS (Fig. 4). These results suggested that PMN-MDSCs subset gain a prognostic value for metastatic PC patients receiving first-line treatment.

Different cell fractions and gene expressions in mHSPC revealed by scRNA-seq analysis

Since the fraction of MDSCs was significantly increased in mHSPC patients, we investigated the immune cell dynamics and gene expressions of MDSCs using an scRNA-seq analysis of PBMCs from a patient with an average percentage increase in the fraction of PMN-MDSCs (Neutrophil; 64.4%, Lymphocyte; 26.3%, Monocyte; 8.4%, e-MDSCs; 1.10%, PMN-MDSCs; 0.79%, M-MDSCs 3.24%) and a healthy volunteer (Neutrophil; 51.6%, Lymphocyte; 43.3%, Monocyte; 3.4%, e-MDSCs; 0.74%, PMN-MDSCs; 0.04%, M-MDSCs 2.76%). The transcripts of cells were obtained by the 10X Genomics platform, and we acquired 21,280 and 21,697 genes of single cells from the subject and control, respectively. Fig.5-A showed the t-SNE plots displaying clusters of all immune cells of the mHSPC patient (3885 cells) and the healthy control (4639 cells). We obtained 14 clusters by unbiased graph-based clustering, and identified cell groups consisting of T cells, B cells, innate immune cells (γδT cells, NK cells, and NKT cells), and myeloid cells. A greater increase in the frequencies of innate immune cells and myeloid cells was shown in the patient than in the

control (Fig. 5-A), and the gene expressions of these immune cells differed among subjects (Suppl. Table 2). For example, the expression of S100 proteins, which relates to the development and progression of various cancers, was increased in the innate immune cells and myeloid cells of the PC patient. We also confirm that the gene expressions were different even in the same cell subset by the reclustering of T cells, innate lymphoid cells and myeloid cells (Supple. Fig. 4). While the population of effecter memory CD4/8 T cells was almost the same between PC patient and control, the ratio of central memory CD4/8 T cells was decreased remarkably in the patient, inferring that the differentiation of T cells into effector cells was enhanced in the tumor-bearing state. Immune checkpoint molecules were not detected as differentially expressed genes in T cell subsets (Suppl. Table 2), whereas the S100 gene-expressing γδT cells and monocytes were increased in the mHSPC sample (Suppl. Fig. 4). In addition, we were able to detect small cell groups of PMN-MDSCs and found the enhanced expression of genes involved in tumor progression (CXCL8, IL-1b, proteoglycan versican (VCAN), and Transforming growth factor b induced (TGFBI)) (Fig. 5-B). While we acknowledge that further data accumulation is needed, our present RNA-seq data were largely consistent with previous reports on other cancers [23, 24], suggesting that these genes could also be potential therapeutic targets in mHSPC.

Discussion

This is the first study that showing the implication of MDSC subsets in the prognostic value for patients with mHSPC. While it has been reported that an expansion of PMN-MDSC and M-MDSC subsets occurred in the peripheral blood and tumor tissue of CRPC [13–16, 25], it was unclear whether PMN-MDSCs has a predictive value in the progress of mHSPC. In this study, we found the elevated proportion of PMN-MDSC fraction were associated with a poor prognosis. In addition, an analysis of the scRNA-seq in the mHSPC subject showed different immune cell subsets and the immunosuppressive gene expression of PMN-MDSCs.

A unique feature of this study is the finding that the PSA-PFS and OS was poorer when the percentage of PMN-MDSCs was above a specific ratio (≥ 0.30%) than when it was below a ratio (< 0.30%). High percentages of MDSCs have been reported to be associated with a poor prognosis in various malignant neoplasms [21, 22, 26]. However, this correlation was found between the cancer prognosis and total MDSC fractions, rather than the three subsets of MDSCs [21, 22]. In addition, while further measures are required to confirm the contribution of MDSCs to the cancer prognosis on how many times the percentage of MDSCs in the target population increases compared to those of responders or healthy individuals, the high ratio of MDSC fractions in earlier studies was defined as a greater than the mean + 2SD of healthy controls [27], with no proper assessment of MDSC subsets or ratios. In the present study, we defined a high percentage of PMN-MDSCs as above 0.30%, which is close to the median value (0.28%) of patients and about three times that of healthy subjects (0.11%), and we found a significant correlation with the prognosis of mHSPC. This method provides useful insights into the importance of determining the distinct ratio of the specific MDSC subset.

It has been shown that high M-MDSC levels are associated with a shorter OS in CRPC, indicating a relationship between M-MDSCs and a poor clinical outcome [13–16, 25]. In this study, while the proportion of M-MDSCs was increased remarkably in patients with mHSPC, there was no significant difference in either the PSA-PFS and OS of patients and the healthy controls. While it has been reported that PD-L1 was highly expressed on M-MDSCs [28], no expression of PD-L1 on M-MDSCs patients was found in our flow cytometric analysis (data not shown). In addition, the administration of an androgen receptor antagonist was shown to raise the immunosuppressive effect of M-MDSCs via glycolysis enhancement in the murine model [29]. The present scRNA-seq analysis also detected only a small number of M-MDSCs in both the patient (10 cells) and the control (2 cells) and the data was not conclusive with regard to the presence or absence of suppressive gene expressions. Although comparative studies between mHSPC and CRPC are needed to clarify the effect of ADT on the inhibitory function of M-MDSCs, it is possible that M-MDSCs grown on mHSPC are less immuno-suppressive before treatment.

Our scRNA-seq results showed the different proportions of immune cells in the mHSPC patient. Despite the obvious limitation of the present data in that it was from the analysis of a representative case, a greater increase in the ratio of γδT cells and monocytes was found in the PC subject than in the control (Fig. 5-A and Suppl. Figure 4). It was reported that γδT cells are involved in the growth of MDSCs and their recruitment to tumor sites [30]. In this study, the patient's γδT cells displayed high expression levels of S100B, PTGDS, ALOX5P and SPON2 genes, which have been shown to implicate in the MDSC differentiation or tumor progression, suggesting that γδT cells affect MDSC characteristics, including its differentiation in PCs with metastasis [31–33]. Classical monocytes have been reported to show an elevated gene expression on fibrin-binding F13A1 [34], and to function as a scaffold for lung cancer metastasis, while intermediate monocytes have been reported to express a scavenger receptor [35], MARCO which is associated with the poor prognosis of various cancers [36]. Since it has been reported that peripheral blood monocyte counts are correlated with TAM infiltration and prognosis in PC patients after prostatectomy [37], further studies are required to clarify whether these above molecules (S100B, PTGDS, ALOX5P, SPON2, and F13A1) are involved in the progress of mHSPC.

In this scRNA-seq analysis, we were able to detect a small number of PMN-MDSCs, which showed augmented expressions of several genes whose appearance is already known in PMN-MDSCs (Fig. 5-B) [38]. For example, CXCL-8 (IL-8) and IL-1β have been shown to promote cancer progression as well as traffic MDSCs to the tumor microenvironment [24, 39]. VCAN and TGBI enhance tumor metastasis [40, 41]. Because PMN-MDSCs help circulating tumor cell extravasation and contribute to the pre-metastatic niche formation [42], it is possible that these highly expressed genes might be implicated in the metastatic status of PCs. On the other hand, our scRNA-seq did not detect a significant difference in the expression of immune checkpoint molecules expressed on T cells and myeloid cells between the mHSPC patient and the control (Suppl. Table 2). While it may be that detection is only possible when data from a number of subjects is accumulated, it also may be that differences in the expression of immune-check point molecules contributed to the finding that those inhibitors are less effective in PCs than other carcinomas.

In conclusion, our present study showed that PMN-MDSCs are correlated with the poor prognosis of patients with mHSPC. The results of an scRNA-seq analysis detected PMN-MDSCs with a high expression gene involved in cancer progress. According to these results, PMN-MDSCs, including their highly expressed genes, have potential as novel therapeutic targets against mHSPC.

Abbreviations

PC = prostate cancer

ADT = androgen deprivation therapy

CRPC = castration resistance prostate cancer

MDSCs = myeloid-derived suppressor cells

PMN-MDSCs = polymorphonuclear myeloid-derived suppressor cells

M-MDSCs = monocytic myeloid-derived suppressor cells

e-MDSCs = early-stage myeloid-derived suppressor cells

MMP-9 = matrix metallopeptidase-9

VEGF = vascular endothelial growth factor

TAMs = tumor associated macrophages

mHSPC = metastatic-hormone sensitive prostate cancer

scRNA-seq = single cell RNA-sequencing

PSA = prostate-specific antigen

ALP = alkaline phosphatase

LDH = lactate dehydrogenase

Hb = hemoglobin

Alb = albumin

CRP = c-reactive protein

PSA-PFS = PSA progression-free survival

Suppl. = supplementary

RBCs = red blood cells

PBMCs = peripheral blood cells

PBS = phosphate-buffered saline

UMI = unique molecular identifier

t-SNE = T-distributed stochastic neighbor embedding

OS = overall survival

VCAN = proteoglycan versican

TGBI = Transforming growth factor b induced

SD = standard deviation

Declarations

Conflict of interests

The authors have no relevant financial or non-financial interests to disclose.

Funding

This work was supported in part by JSPS KAKENHI Grant Number 19K07511 to K.T., 19K06471 to T. K., and 20K09719 to A.N.

Statements & Declarations:

All authors contributed to the study conception and design. Conceptualization was performed by Yuki Kohada, Akito Kuromoto, Akira Nakamura, and Makoto Sato. Material preparation, data collection and analysis were performed by Yuki Kohada, Akito Kuromoto, Kazuya Takeda, Hiromichi Iwamura, Yuri Atobe, Jun Ito, Tomonori Kaifu, and Akira Nakamura. The first draft of the manuscript was written by Yuki Kohada. The review and editing of the manuscript were performed by Akira Nakamura. Supervision was provided by Yasuhiro Kaiho, Ichiro Nakashima, Nobuyuki Hinata, Akira Nakamura, and Makoto Sato. All authors commented on previous versions of the manuscript, and read and approved the final manuscript.

The datasets generated during and/or analyzed during the current study are available from the corresponding author on reasonable request.

This study was performed in line with the principles of the Declaration of Helsinki. This study had been approved by clinical research ethics boards of Tohoku Medical and Pharmaceutical Hospital (approval number: 2018-2-062).

Written informed consent was obtained from all the parents.

The authors affirm that human research participants provided informed consent for publication of the images in Figures 1 and 5, and Supplementary Figure 4.

References

1. Siegel RL, Miller KD, Fuchs HE, Jemal A (2021) Cancer Statistics, 2021. CA Cancer J Clin. 71: 7–33. doi: 10.3322/caac.21654
2. Mohler JL, Armstrong AJ, Bahnson RR et al. (2016) Prostate Cancer, Version 1.2016. J Natl Compr Canc Netw. 14: 19–30. doi: 10.6004/jnccn.2016.0004
3. Armstrong AJ, Szmulewitz RZ, Petrylak DP et al. (2019) ARCHES: A Randomized, Phase III Study of Androgen Deprivation Therapy With Enzalutamide or Placebo in Men With Metastatic Hormone-Sensitive Prostate Cancer. J Clin Oncol. 37: 2974–86. doi: 10.1200/JCO.19.00799
4. Kim TJ, Koo KC (2020) Current Status and Future Perspectives of Checkpoint Inhibitor Immunotherapy for Prostate Cancer: A Comprehensive Review. Int J Mol Sci. 21. doi: 10.3390/ijms21155484
5. Kantoff PW, Higano CS, Shore ND et al. (2010) Sipuleucel-T immunotherapy for castration-resistant prostate cancer. N Engl J Med. 363: 411–22. doi: 10.1056/NEJMoa1001294
6. Gabrilovich DI, Bronte V, Chen SH, Colombo MP, Ochoa A, Ostrand-Rosenberg S, Schreiber H (2007) The terminology issue for myeloid-derived suppressor cells. Cancer Res. 67: 425; author reply 6. doi: 10.1158/0008-5472.CAN-06-3037
7. Bronte V, Brandau S, Chen SH et al. (2016) Recommendations for myeloid-derived suppressor cell nomenclature and characterization standards. Nat Commun. 7: 12150. doi: 10.1038/ncomms12150
8. Zhou J, Nefedova Y, Lei A, Gabrilovich D (2018) Neutrophils and PMN-MDSC: Their biological role and interaction with stromal cells. Semin Immunol. 35: 19–28. doi: 10.1016/j.smim.2017.12.004
9. Tcyganov E, Mastio J, Chen E, Gabrilovich DI (2018) Plasticity of myeloid-derived suppressor cells in cancer. Curr Opin Immunol. 51: 76–82. doi: 10.1016/j.coi.2018.03.009
10. Khan ANH, Emmons TR, Wong JT et al. (2020) Quantification of Early-Stage Myeloid-Derived Suppressor Cells in Cancer Requires Excluding Basophils. Cancer Immunol Res. 8: 819–28. doi: 10.1158/2326-6066.CIR-19-0556
11. Cui C, Lan P, Fu L (2021) The role of myeloid-derived suppressor cells in gastrointestinal cancer. Cancer Commun (Lond). 41: 442–71. doi: 10.1002/cac2.12156
12. Yang Z, Guo J, Weng L, Tang W, Jin S, Ma W (2020) Myeloid-derived suppressor cells-new and exciting players in lung cancer. J Hematol Oncol. 13: 10. doi: 10.1186/s13045-020-0843-1
13. Hossain DM, Pal SK, Moreira D et al. (2015) TLR9-Targeted STAT3 Silencing Abrogates Immunosuppressive Activity of Myeloid-Derived Suppressor Cells from Prostate Cancer Patients. Clin Cancer Res. 21: 3771–82. doi: 10.1158/1078-0432.CCR-14-3145

14. Idorn M, Kollgaard T, Kongsted P, Sengelov L, Thor Straten P (2014) Correlation between frequencies of blood monocytic myeloid-derived suppressor cells, regulatory T cells and negative prognostic markers in patients with castration-resistant metastatic prostate cancer. Cancer Immunol Immunother. 63: 1177–87. doi: 10.1007/s00262-014-1591-2
15. Chi N, Tan Z, Ma K, Bao L, Yun Z (2014) Increased circulating myeloid-derived suppressor cells correlate with cancer stages, interleukin-8 and – 6 in prostate cancer. Int J Clin Exp Med. 7: 3181–92.
16. Vuk-Pavlovic S, Bulur PA, Lin Y, Qin R, Szumlanski CL, Zhao X, Dietz AB (2010) Immunosuppressive CD14 + HLA-DRlow/- monocytes in prostate cancer. Prostate. 70: 443–55. doi: 10.1002/pros.21078
17. Scher HI, Morris MJ, Stadler WM et al. (2016) Trial Design and Objectives for Castration-Resistant Prostate Cancer: Updated Recommendations From the Prostate Cancer Clinical Trials Working Group 3. J Clin Oncol. 34: 1402–18. doi: 10.1200/JCO.2015.64.2702
18. Wang S, Tan Q, Hou Y, Dou H (2021) Emerging Roles of Myeloid-Derived Suppressor Cells in Diabetes. Front Pharmacol. 12: 798320. doi: 10.3389/fphar.2021.798320
19. Ortiz ML, Lu L, Ramachandran I, Gabrilovich DI (2014) Myeloid-derived suppressor cells in the development of lung cancer. Cancer Immunol Res. 2: 50–8. doi: 10.1158/2326-6066.CIR-13-0129
20. Sawant A, Deshane J, Jules J, Lee CM, Harris BA, Feng X, Ponnazhagan S (2013) Myeloid-Derived Suppressor Cells Function as Novel Osteoclast Progenitors Enhancing Bone Loss in Breast Cancer. Cancer Res. 73: 672–82. doi: 10.1158/0008-5472.
21. Yang G, Shen W, Zhang Y, Liu M, Zhang L, Liu Q, Lu HH, Bo J (2017) Accumulation of myeloid-derived suppressor cells (MDSCs) induced by low levels of IL-6 correlates with poor prognosis in bladder cancer. Oncotarget. 8: 38378–88. doi: 10.18632/oncotarget.16386
22. Wang L, Chang EW, Wong SC, Ong SM, Chong DQ, Ling KL (2013) Increased myeloid-derived suppressor cells in gastric cancer correlate with cancer stage and plasma S100A8/A9 proinflammatory proteins. J Immunol. 190: 794–804. doi: 10.4049/jimmunol.1202088
23. Cedervall J, Zhang Y, Olsson AK (2016) Tumor-Induced NETosis as a Risk Factor for Metastasis and Organ Failure. Cancer Res. 76: 4311–5. doi: 10.1158/0008-5472.CAN-15-3051
24. Groth C, Weber R, Lasser S, Ozbay FG, Kurzay A, Petrova V, Altevogt P, Utikal J, Umansky V (2021) Tumor promoting capacity of polymorphonuclear myeloid-derived suppressor cells and their neutralization. Int J Cancer. 149: 1628–38. doi: 10.1002/ijc.33731
25. Wen J, Huang G, Liu S et al. (2020) Polymorphonuclear MDSCs are enriched in the stroma and expanded in metastases of prostate cancer. J Pathol Clin Res. 6: 171–7. doi: 10.1002/cjp2.160
26. Gao XH, Tian L, Wu J et al. (2017) Circulating CD14(+) HLA-DR(-/low) myeloid-derived suppressor cells predicted early recurrence of hepatocellular carcinoma after surgery. Hepatol Res. 47: 1061–71. doi: 10.1111/hepr.12831
27. de Goeje PL, Bezemer K, Heuvers ME et al. (2015) Immunoglobulin-like transcript 3 is expressed by myeloid-derived suppressor cells and correlates with survival in patients with non-small cell lung cancer. Oncoimmunology. 4: e1014242. doi: 10.1080/2162402X.2015.1014242

28. Okla K, Rajtak A, Czerwonka A, Bobinski M, Wawruszak A, Tarkowski R, Bednarek W, Szumilo J, Kotarski J (2020) Accumulation of blood-circulating PD-L1-expressing M-MDSCs and monocytes/macrophages in pretreatment ovarian cancer patients is associated with soluble PD-L1. J Transl Med. 18: 220. doi: 10.1186/s12967-020-02389-7
29. Zhao Y, Peng X, Baldwin H, Zhang C, Liu Z, Lu X (2021) Anti-androgen therapy induces transcriptomic reprogramming in metastatic castration-resistant prostate cancer in a murine model. Biochim Biophys Acta Mol Basis Dis. 1867: 166151. doi: 10.1016/j.bbadis.2021.166151
30. Park JH, Lee HK (2021) Function of gammadelta T cells in tumor immunology and their application to cancer therapy. Exp Mol Med. 53: 318–27. doi: 10.1038/s12276-021-00576-0
31. Charmsaz S, Hughes E, Bane FT et al. (2017) S100beta as a serum marker in endocrine resistant breast cancer. BMC Med. 15: 79. doi: 10.1186/s12916-017-0836-2
32. Trabanelli S, Chevalier MF, Martinez-Usatorre A et al. (2017) Tumour-derived PGD2 and NKp30-B7H6 engagement drives an immunosuppressive ILC2-MDSC axis. Nat Commun. 8: 593. doi: 10.1038/s41467-017-00678-2
33. Schmid F, Wang Q, Huska MR et al. (2016) SPON2, a newly identified target gene of MACC1, drives colorectal cancer metastasis in mice and is prognostic for colorectal cancer patient survival. Oncogene. 35: 5942–52. doi: 10.1038/onc.2015.451
34. Porrello A, Leslie PL, Harrison EB et al. (2018) Factor XIIIA-expressing inflammatory monocytes promote lung squamous cancer through fibrin cross-linking. Nat Commun. 9: 1988. doi: 10.1038/s41467-018-04355-w
35. Kiss M, Caro AA, Raes G, Laoui D (2020) Systemic Reprogramming of Monocytes in Cancer. Front Oncol. 10: 1399. doi: 10.3389/fonc.2020.01399
36. Shi B, Chu J, Huang T, Wang X, Li Q, Gao Q, Xia Q, Luo S (2021) The Scavenger Receptor MARCO Expressed by Tumor-Associated Macrophages Are Highly Associated With Poor Pancreatic Cancer Prognosis. Front Oncol. 11: 771488. doi: 10.3389/fonc.2021.771488
37. Hayashi T, Fujita K, Nojima S et al. (2017) Peripheral blood monocyte count reflecting tumor-infiltrating macrophages is a predictive factor of adverse pathology in radical prostatectomy specimens. Prostate. 77: 1383–8. doi: 10.1002/pros.23398
38. Veglia F, Perego M, Gabrilovich D (2018) Myeloid-derived suppressor cells coming of age. Nat Immunol. 19: 108–19. doi: 10.1038/s41590-017-0022-x
39. Yang Y, Li C, Liu T, Dai X, Bazhin AV (2020) Myeloid-Derived Suppressor Cells in Tumors: From Mechanisms to Antigen Specificity and Microenvironmental Regulation. Front Immunol. 11: 1371. doi: 10.3389/fimmu.2020.01371
40. Wang Z, Li Z, Wang Y et al. (2015) Versican silencing improves the antitumor efficacy of endostatin by alleviating its induced inflammatory and immunosuppressive changes in the tumor microenvironment. Oncol Rep. 33: 2981–91. doi: 10.3892/or.2015.3903
41. Lakshmanachetty S, Cruz-Cruz J, Hoffmeyer E, Cole AP, Mitra SS (2021) New Insights into the Multifaceted Role of Myeloid-Derived Suppressor Cells (MDSCs) in High-Grade Gliomas: From

Metabolic Reprograming, Immunosuppression, and Therapeutic Resistance to Current Strategies for Targeting MDSCs. Cells. 10. doi: 10.3390/cells10040893

42. Trovato R, Cane S, Petrova V, Sartoris S, Ugel S, De Sanctis F (2020) The Engagement Between MDSCs and Metastases: Partners in Crime. Front Oncol. 10: 165. doi: 10.3389/fonc.2020.00165

Tables

Table 1. Baseline characteristics

Variables	All patients
	n = 31
Age (years): median (range)	73 (63–84)
Diabetes	
no	22 (71.0)
yes	9 (29.0)
Status of smoking	
non-smoker	11 (35.5)
current or past smoker	20 (64.5)
Gleason score: n (%)	
8	13 (41.9)
9, 10	18 (58.1)
Prostate-specific antigen (ng/mL): median (range)	224.0 (2.7–10116.0)
Alkaline phosphatase (IU/L): median (range)	298.0 (104.0–1910.0)
Lactate dehydrogenase (IU/L): median (range)	198.0 (144.0–432.0)
Hemoglobin (g/dL): median (range)	13.6 (9.8–15.6)
Albumin (g/dL): median (range)	4.0 (3.1–4.6)
White blood cell (/μL): median (range)	5300 (1400–9400)
Neutrophil (%): median (range)	63.4 (46.2–80.0)
Lymphocyte (%): median (range)	25.8 (12.9–43.1)
Monocyte (%): median (range)	7.1 (4.5–14.0)
Eosinophil (%): median (range)	1.8 (0.1–6.7)
Basophil (%): median (range)	0.7 (0.0–1.5)
Neutrophil-lymphocyte ratio: median (range)	2.45 (1.27–6.20)

Figures

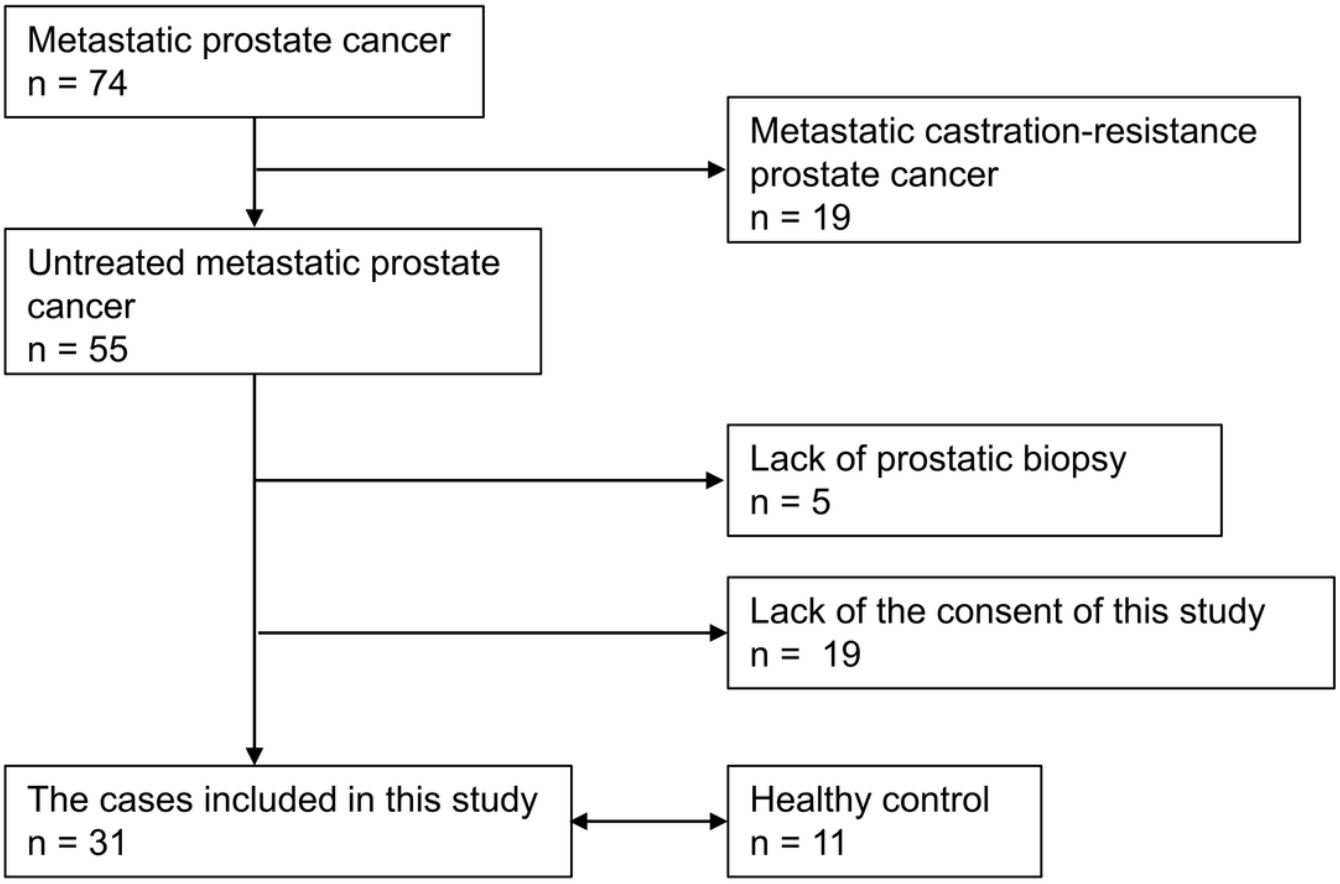

Figure 1

Selective strategy of patients with mHSPC in this study

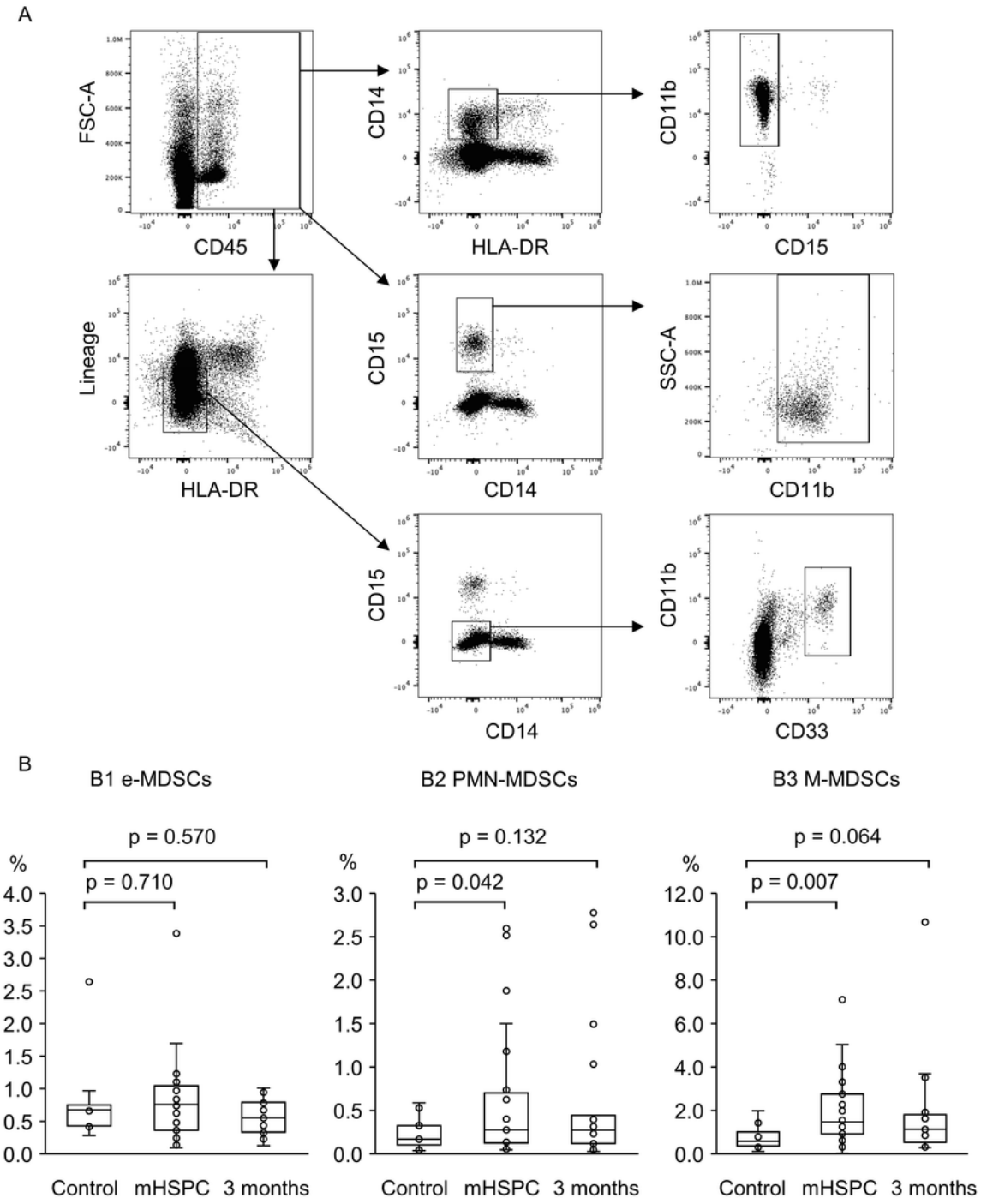

Figure 2

A: Gating strategy for the identification of peripheral MDSC subsets of the mHSPC patient by Flow cytometry. Each of the MDSC subsets listed below was detected in the cell fraction excluding CD45-negative cells (RBCs and endothelial cells). M-MDSCs; $CD11b^{+}CD15^{-}CD14^{+}HLA\text{-}DR^{-}$ cells, PMN-MDSCs; $CD11b^{+}CD14^{-}$ $CD15^{+}$ cells, e-MDSCs; $CD11b^{+}CD33^{+}CD15^{-}CD14^{-}Lineage\ (CD3/19/56)^{-}HLA\text{-}DR^{-}$ cells. B: A comparing of the percentage of each of the MDSC subsets of the healthy control, pretreated mHSPC

patients, and those treated by ADT for 3 months. B1. e-MDSCs, healthy control; median 0.67%, range 0.28–2.64%, mHSPC; median 0.76%, range 0.09–3.38%, 3 months; median 0.57%, range 0.13–1.01%, B2. PMN-MDSCs, healthy control; median 0.11%, range 0.04–0.53%, mHSPC; median 0.28%, range 0.05–2.60%, 3 months; median 0.25%, range 0.03–2.76%, B3. M-MDSCs, healthy control; median 0.58%, range 0.11–1.98%, mHSPC; median 1.46%, range 0.01–7.10%, 3 months; median 1.20%, range 0.29–10.67%. MDSCs; myeloid-derived suppressor cells, mHSPC; metastatic-hormone sensitive prostate cancer, PMN-MDSCs; polymorphonuclear MDSCs, M-MDSCs; monocytic MDSCs, e-MDSCs; early-stage MDSCs

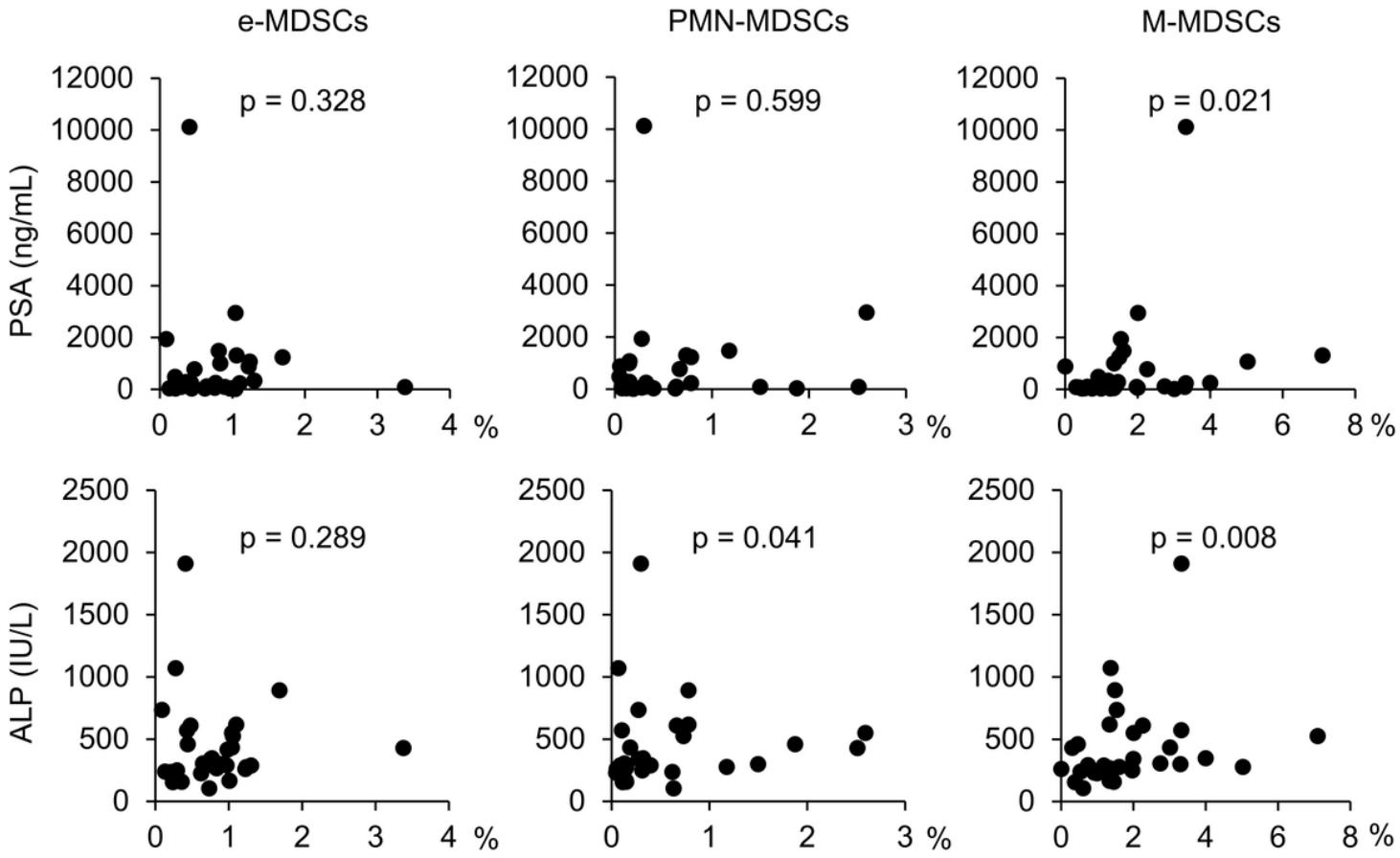

Figure 3

Relevance between each MDSC subset and PSA and ALP. MDSCs; myeloid-derived suppressor cells, PMN-MDSCs; polymorphonuclear MDSCs, M-MDSCs; monocytic MDSCs, e-MDSCs; early-stage MDSCs, PSA; prostate-specific antigen, ALP; alkaline phosphatase

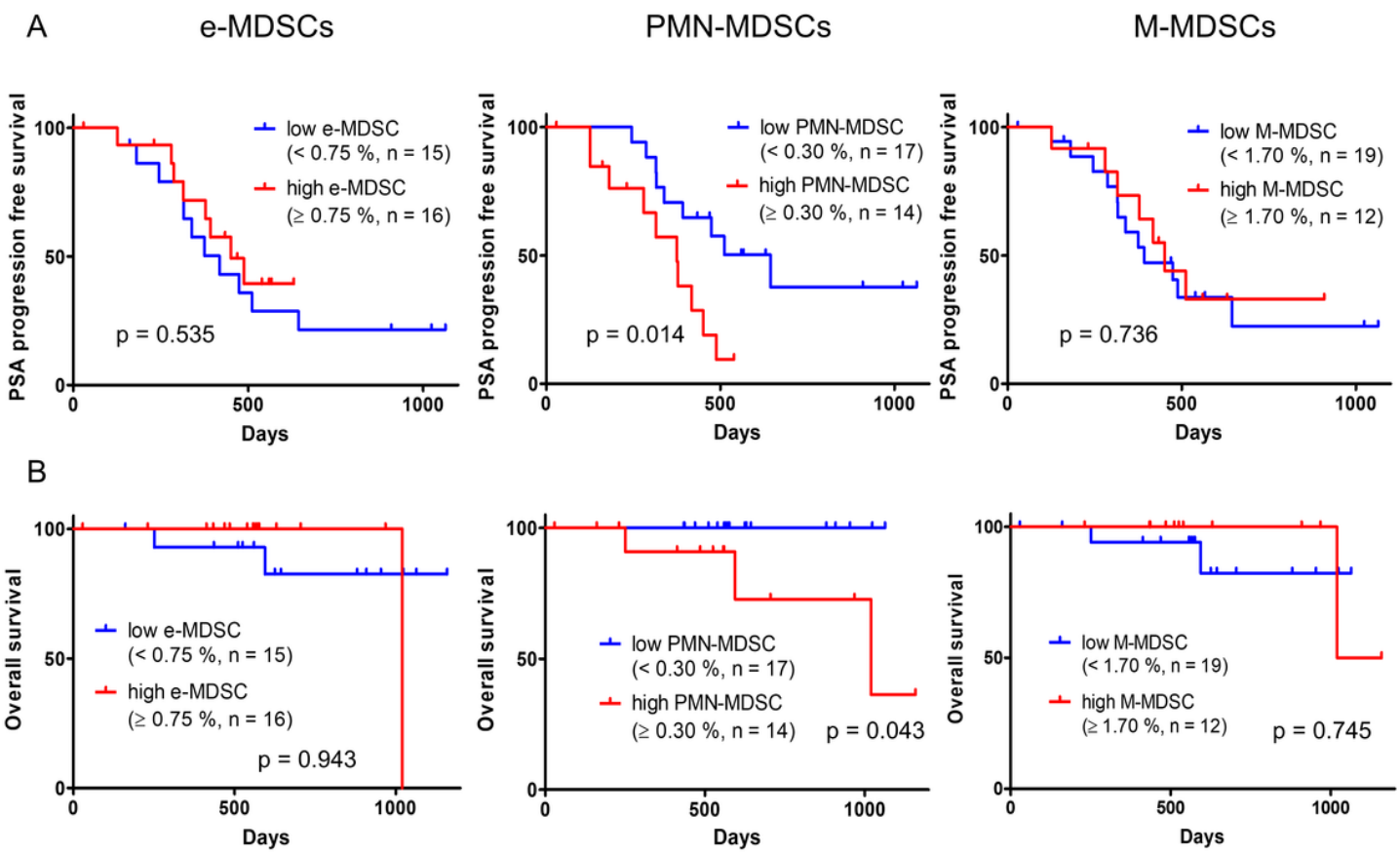

Figure 4

Kaplan–Meier curve of PSA– progression free survival (A) and OS (B) in patients with high and low percentages of each MDSC fraction. PSA; prostate-specific antigen, OS; overall survival, MDSCs; myeloid-derived suppressor cells, PMN-MDSCs; polymorphonuclear MDSCs, M-MDSCs; monocytic MDSCs, e-MDSCs; early-stage MDSCs

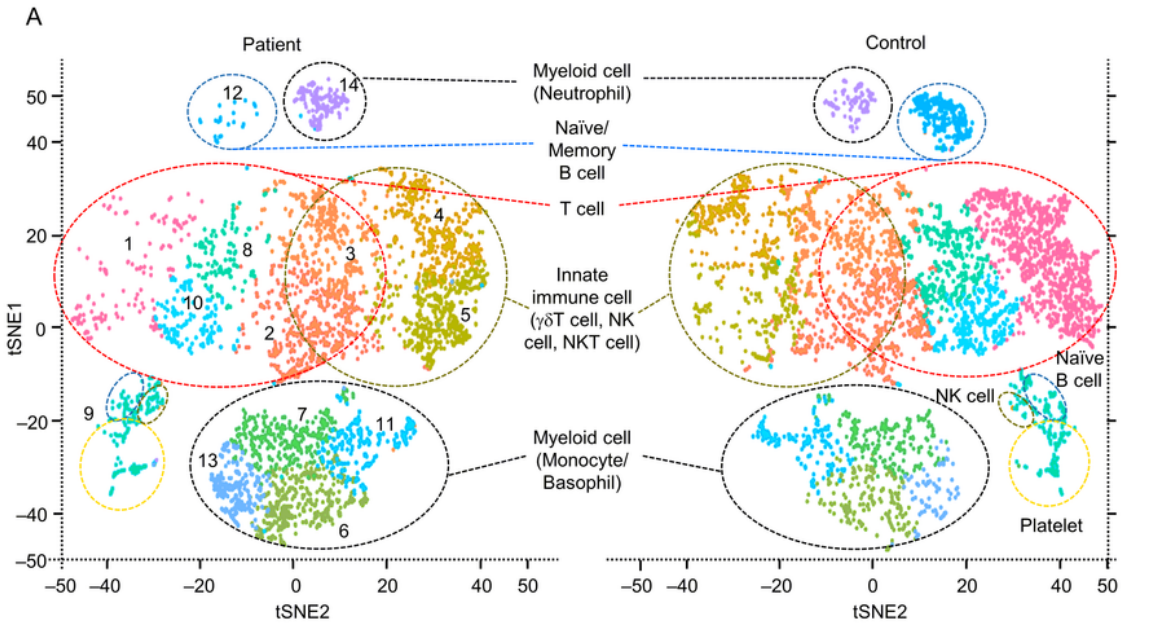

Cluster No.	Representative types of cells in each cluster	Count of the patient	Count of the control	Cluster No.	Representative types of cells in each cluster	Count of the patient	Count of the contro
Cluster 1	Central memory CD4T and CD8T cells	132	1171	Cluster 8	Effector memory CD4T cells, Central memory CD8T cells, CD4CD8DN T cells, NKT cells, and γδ T cells	127	199
Cluster 2	Effector memory CD8T and CD4T cells, γδ T cells and NK cells	540	617	Cluster 9	Naive B cells, NK cells and Platelets	201	257
Cluster 3	Effector memory CD8T cells, CD4T cells, and γδ T cells	359	473	Cluster 10	Central memory/Effector memory CD4 and CD8T cells, CD4CD8DN T cells and NKT cells	132	299
Cluster 4	γδ T cells and NK cells	468	346	Cluster 11	Neutrophils, intermediate monocytes and basophils	241	172
Cluster 5	γδ T cell and NK cells	513	248	Cluster 12	Naive/Memory B cells	25	308
Cluster 6	Classical/intermediate Monocytes and Neutrophils	399	185	Cluster 13	Classical/intermediate Monocytes	231	68
Cluster 7	Classical Momocytes/Neutrophils	348	199	Cluster 14	Neutrophils and PMN-MDSCs	169	97

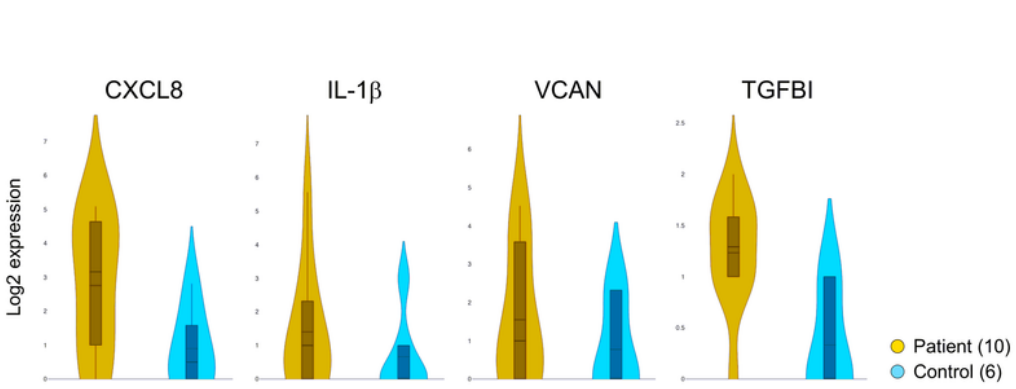

Figure 5

A. t-SNE plot showing clusters of all immune and non-immune cells of both the mHSPC patient and the healthy control generated from 10X Genomics platform. Cell fractions identified for each cluster and their counts are shown. B. Violin plots showing the elevated genes of secreted proteins in the patient PMN-MDSCs compared with that of the healthy control. t-SNE; T-distributed stochastic neighbor embedding, mHSPC; metastatic-hormone sensitive prostate cancer, PMN-MDSCs; poly-morphonuclear MDSCs

Supplementary Files

This is a list of supplementary files associated with this preprint. Click to download.

- SuppleTable1.xlsx
- SuppleTable2.xlsx
- SupplementaryFigure1.tif
- SupplementaryFigure2.tif
- SupplementaryFigure3.tif
- SupplementaryFigure4.tif